

# Single-File Diffusion of Protein Drugs through Cylindrical Nanochannels

Seung Yun Yang,<sup>†,‡</sup> Jeong-A Yang,<sup>\*,‡</sup> Eung-Sam Kim,<sup>§</sup> Gumhye Jeon,<sup>†</sup> Eun Ju Oh,<sup>‡</sup> Kwan Yong Choi,<sup>§</sup> Sei Kwang Hahn,<sup>\*,\*</sup> and Jin Kon Kim<sup>†,\*</sup>

<sup>†</sup>National Creative Research Center for Block Copolymer Self-Assembly, Departments of Environmental Science & Engineering and Chemical Engineering, <sup>‡</sup>Department of Materials Science & Engineering, and <sup>§</sup>Department of Life Science and School of Inter-disciplinary Bioscience and Bioengineering, Pohang University of Science and Technology, Kyungbuk 790-784, Korea. <sup>‡</sup>These authors contributed equally to this work.

Controlled and long-term protein drug delivery has been considered as one of the most promising biomedical applications of nanotechnology.<sup>1</sup> A wide range of materials and devices have been developed for the delivery of protein drugs in a controlled manner within a therapeutic range.<sup>2,3</sup> However, conventional technologies were not successful due to the protein denaturation during and after the formulation. Although various protein conjugates with polyethyleneglycol (PEG) have been successfully commercialized as once a week injection formulations, there is no controlled release depot system in the market for protein drugs lasting for longer than a week.

A critical challenge in long-term controlled delivery of protein drugs is to maintain the integrity of highly sensitive tertiary structure and the therapeutic efficacy of protein drugs in physiological condition for long periods.<sup>4–6</sup> Once protein drugs are denatured, they not only are therapeutically inactive but also cause unpredictable side effects such as inflammation, toxicity, and immune responses.<sup>2,3</sup> For instance, despite the successful commercialization of a controlled release system of human growth hormone (hGH) using poly(lactic-co-glycolic acid) (PLGA) microparticles under a trade-name of Nutropin Depot, it was withdrawn from the market due to the protein denaturation by hydrophobic interaction and/or harsh acidic microenvironments caused by the degradation of PLGA inside the body.<sup>7</sup>

The best long-term controlled delivery system of protein drugs without denaturation might be possible by exploiting the passive diffusion through a membrane without physical and chemical stresses. This can be achieved when pore sizes in a

**ABSTRACT** A new drug delivery device using cylindrical block copolymer nanochannels was successfully developed for controlled protein drug delivery applications. Depending on the hydrodynamic diameter of the protein drugs, the pore size in cylindrical nanochannels could be controlled precisely down to 6 nm by Au deposition. Zero-order release of bovine serum albumin (BSA) and human growth hormone (hGH) by single-file diffusion, which has been observed for gas diffusion through zeolite pores, was realized up to 2 months without protein denaturation. Furthermore, a nearly constant *in vivo* release of hGH from the drug delivery nanodevice implanted to Sprague–Dawley (SD) rats was continued up to 3 weeks, demonstrating the feasibility for long-term controlled delivery of therapeutic protein drugs.

**KEYWORDS:** protein drug · nanochannels · block copolymer · single-file diffusion · controlled drug delivery

membrane are controlled to satisfy the single-file diffusion (SFD)<sup>8,9</sup> condition of protein drugs. SFD was previously observed for the diffusion of CF<sub>4</sub> gas through the pores in zeolites.<sup>8</sup> When pore sizes are carefully adjusted so that two or more diffusing molecules are not allowed to pass through the pores simultaneously, protein drugs are released by SFD through the membrane without initial burst by the Fickian diffusion. The release rate of a protein drug becomes constant with time irrespective of its concentration in the reservoirs. This phenomenon is analogous to the constant dropping rate of sands through an hour-glass with time, although the mechanism is fairly different. Ferrari and co-workers<sup>10–13</sup> prepared a nanoporous silicon membrane by multiple steps including micropattern fabrication by photolithography, the deposition of the sacrificial SiO<sub>2</sub> layer, back etching, and removal of the SiO<sub>2</sub> layer. They confirmed controlled *in vitro* release of insulin and IgG antibody<sup>11</sup> when the sizes of the nanochannels in the membrane were carefully controlled. Later, they showed the constant release of labeled bovine serum albumin (BSA) during *in vitro* and *in vivo* tests.<sup>12</sup>

See the accompanying Perspective by Jackson and Hillmyer on p 3548.

\*Address correspondence to jkkim@postech.ac.kr, skhanb@postech.ac.kr.

Received for review March 7, 2010 and accepted May 16, 2010.

Published online May 27, 2010. 10.1021/nn100464u

© 2010 American Chemical Society

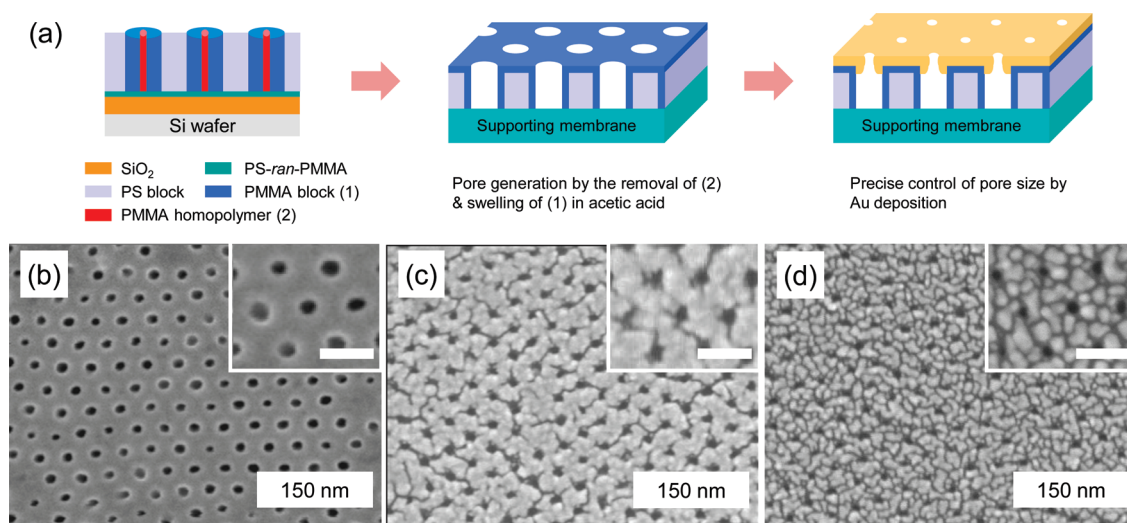


**Figure 1.** (a) Schematics for the preparation of block copolymer membrane with cylindrical nanochannels. The mixture of PS-*b*-PMMA/PMMA solution in toluene was spin-coated on a modified silicon wafer. The film was floated onto a supporting membrane by dissolving the silicon oxide layer from the substrate (the left image). Then cylindrical pores were generated by the removal of PMMA homopolymer and swelling of PMMA block in acetic acid (the middle image). Pore sizes in the nanoporous membrane were controlled more precisely by Au deposition according to the hydrodynamic diameter of a target protein drug (the right image). (b–d) FE-SEM images of the top surface with a different Au deposition thickness: (b) 0 nm (before Au deposition), (c) 7 nm, and (d) 11 nm. The average pore size decreased from ca. 15 nm to ca. 10 nm and ca. 6 nm. Scale bars in the inset correspond to 30 nm.

However, multiple and complicated steps were needed for the fabrication of nanoporous silicon membrane. Moreover, the concept of SFD through a membrane could not be fully demonstrated because the membranes have rectangular pores where only one dimension is nanometer-sized with the other dimension in micrometer-scale. Despite the constant *in vitro* release of lysozyme, *in vivo* application was not successful.<sup>13</sup> Another nanoporous membrane having unidimensional pores was prepared by pattern transfer, rapid thermal annealing, self-assembling, and anodizing methods. However, a constant release based on single-file diffusion was not fully demonstrated using the membrane.<sup>14–22</sup>

In this work, a new drug delivery device was developed containing a unique membrane with cylindrical nanochannels prepared by the self-assembly of polystyrene-*block*-poly(methylmethacrylate) copolymer (PS-*b*-PMMA). The pore size in the membrane was carefully tuned from 15 to 6 nm by the control of Au deposition time. We observed a long-term and constant *in vitro* release of both BSA and hGH without denaturation by SFD up to 2 months. We also demonstrated the feasibility of *in vivo* applications to long-term controlled delivery of hGH. The novel protein drug delivery device system using cylindrical block copolymer nanochannels was discussed for the application to the treatment of various chronic diseases requiring painful frequent injection.

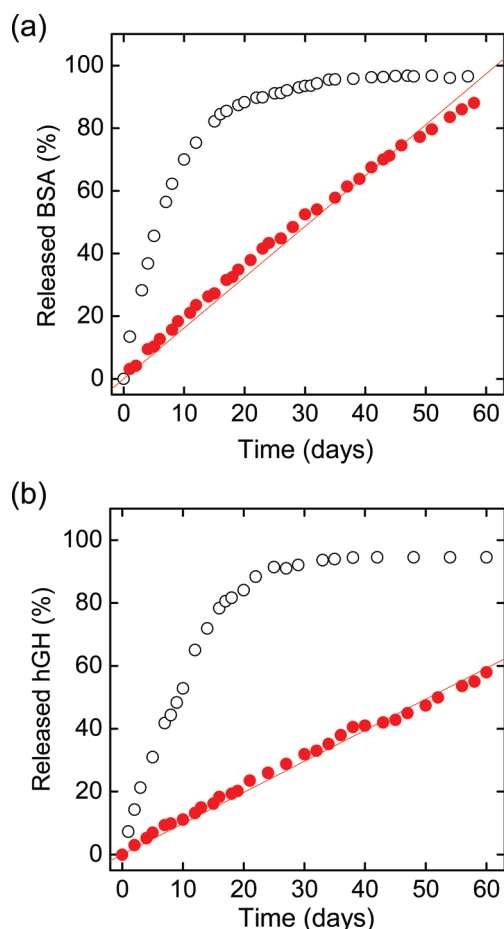
## RESULTS AND DISCUSSION

Figure 1a shows schematics for the fabrication of nanoporous membranes with cylindrical nanochannels.

The upper layer with a thickness of 80 nm was prepared using a thin film of the mixture of PS-*b*-PMMA having cylindrical microdomains of PMMA and PMMA homopolymer on a silicon oxide layer. As previously reported elsewhere,<sup>23</sup> the cylindrical microdomains in the film were oriented vertically to a silicon substrate with an energetically neutral brush (the left image in Figure 1a). This film was floated from the substrate in a buffered HF solution and transferred onto a microfiltration polysulfone membrane acting as a supporting layer. Cylindrical nanochannels in the upper layer were generated by selective removal of the PMMA homopolymer in the cylindrical PMMA microdomains with acetic acid. At the same time, the PMMA block migrated onto the PS matrix by swelling in acetic acid (the middle image in Figure 1a). The resulting membrane had the well-ordered array of vertically aligned cylindrical nanochannels with a narrow pore size distribution. We could control precisely the pore size by Au deposition (the right image in Figure 1a). During the Au deposition, some Au was also deposited on the wall of the pores as well as on the top of the upper layer of the membrane. Thus, the pore size decreased with increasing the thickness of the Au deposition layer on the membrane. Although the pore size also decreased by the deposition of other metals (for instance, Ti or Al), Au was chosen because of its good biocompatibility<sup>24</sup> and excellent adhesion with the membrane. Figure 1b–d shows field-emission scanning electron microscopy (FE-SEM) images for the top surface of the nanoporous membrane with different Au deposition thicknesses. Cylindrical pores with a diameter of ca. 15 nm were uniformly formed in the nanoporous membrane, as shown

in Figure 1b. Pore size decreased with increasing the Au deposition layer. For instance, at a Au deposition layer with 7 nm thickness, the average diameter of nanopores became *ca.* 10 nm (Figure 1c). With further increase of Au layer to 11 nm thickness, the diameter of the pores at the top of the membrane was reduced to 6 nm, as shown in Figure 1d. Narrow size distribution of pores was maintained, and vertical nanochannels were preserved after Au deposition (see Figure S1 in the Supporting Information).

A nanoporous membrane with an average pore diameter of 15 nm was used for the delivery of BSA with a molecular weight (MW) of 66 000 Da and a hydrodynamic diameter of *ca.* 8 nm,<sup>12</sup> while another membrane with a pore diameter of 6 nm was employed for the delivery of hGH with a MW of 22 000 Da and a hydrodynamic diameter of *ca.* 3.4 nm.<sup>25</sup> A good adhesion between the Au layer and nanoporous block copolymer film was maintained even after *in vitro* and *in vivo* release tests of the protein drugs up to 2 months. Controlled release of protein drugs based on the single-file diffusion was assessed using a drug delivery device described in Figure S2 of the Supporting Information. Two kinds of proteins (BSA and hGH) were selected as model protein drugs for *in vitro* release tests. Figure 2a shows the *in vitro* release profile of BSA through two different membranes in the drug delivery device. Open and closed circles represent the released BSA amount from the supporting polysulfone membrane having a nominal pore size of 200 nm and the nanoporous block copolymer (BCP) membrane with a pore size of *ca.* 15 nm, respectively. The constant release profile of BSA, which is the case of SFD, was obtained for the BCP membrane, whereas a typical Fickian diffusion release profile was observed for the supporting polysulfone membrane. The results are quite reasonable because the SFD of a protein drug is made possible when the diameter of the cylindrical pores in the membrane is less than twice the hydrodynamic diameter of the protein drug. In this situation, two protein drug molecules cannot pass simultaneously through the pores. The protein release rate could be easily controlled by changing the thickness of the BCP membrane (Figure S3 in the Supporting Information). For the case of hGH with a hydrodynamic diameter of 3.4 nm, however, a BCP membrane with a pore size of *ca.* 15 nm showed a non-linear release, that is, a typical Fickian diffusion (open circles in Figure 2b). Constant release of hGH was observed up to 2 months for a Au-deposited BCP membrane with a pore size of *ca.* 6 nm, approximately 1.7 times larger than the hydrodynamic diameter of hGH (closed circles in Figure 2b). Constant release of hGH was observed until the end of the *in vitro* test ( $\sim 90$  days). From the results, Au deposition was thought to be an effective means to control the pore size of cylindrical nanochannels. In addition, the Au deposition appeared to reduce protein fouling to the polymeric



**Figure 2.** (a) *In vitro* release profile of BSA through the supporting membrane with a nominal pore size of 200 nm (○) and the nanoporous block copolymer membrane with a pore size of 15 nm (red circle). (b) *In vitro* release profile of hGH through the nanoporous membrane with a pore size of 15 nm (○) and Au-deposited nanoporous membrane with a pore size of 6 nm (red circle).

membrane, especially when erythropoietin (EPO) with a high affinity to polymer surface was used (Figure S4 in the Supporting Information).

The intactness of *in vitro* released hGH was assessed by reverse-phase high-performance liquid chromatography (RP-HPLC), sodium dodecyl sulfate–polyacrylamide gel electrophoresis (SDS–PAGE), circular dichroism (CD), and enzyme-linked immunosorbent assay (ELISA). The uniform peak shape with a constant retention time on RP-HPLC of the released hGH samples partially supported that there was no protein denaturation during the *in vitro* release tests (Figure 3a). SDS–PAGE also confirmed that the released hGH was intact with negligible hGH denaturation. The released hGH even after 60 days was detected at almost the same position with intact hGH having a molecular weight of 22 kDa (Figure 3b). CD spectra of the released hGH after 30 and 60 days were identical to that of hGH in stock solution, indicating that the secondary structure of hGH was maintained (Figure 3c). All of these results supported that the diffusion

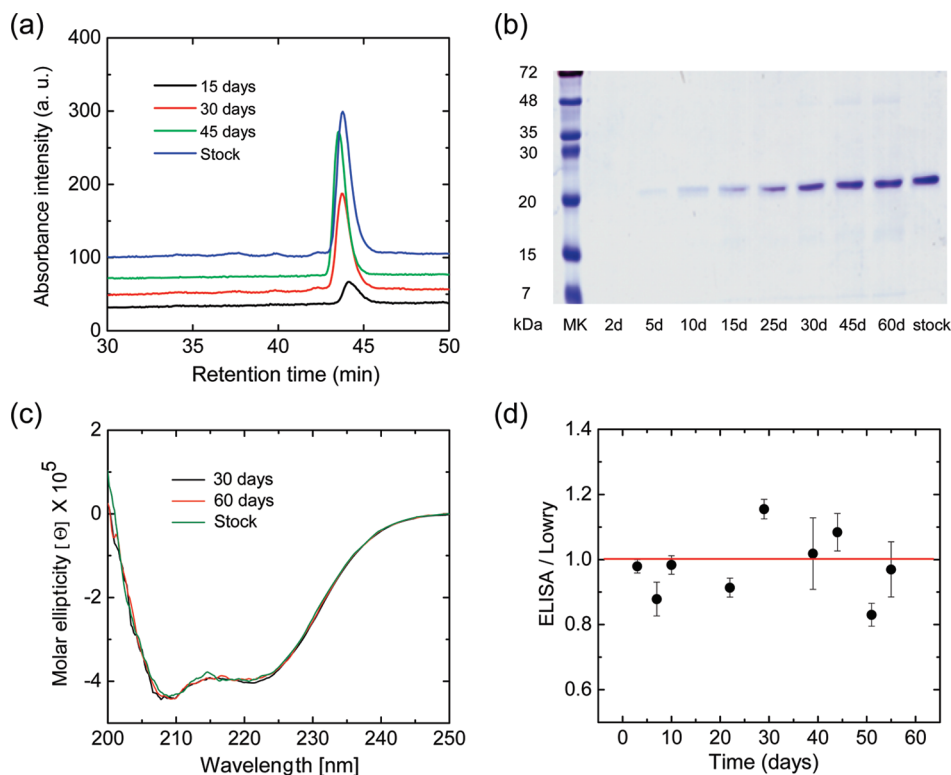


**Figure 3.** Characterization of *in vitro* released hGH. (a) RP-HPLC of hGH stock solution, and *in vitro* released hGH after 15, 30, and 45 days. (b) SDS-PAGE (100 V, 25 °C) of hGH stock solution and *in vitro* released hGH up to 60 days. (c) Far-UV CD spectra of hGH stock solution and *in vitro* released hGH in PBS (pH 7.4, 25 °C) after 30 and 60 days. CD results were expressed as a molar ellipticity in mdeg · cm<sup>2</sup>/decimole using a molecular weight of 22 kDa, a path length of 0.2 cm, and the concentration of each sample in g/cm<sup>3</sup>. (d) Ratio of *in vitro* released hGH concentrations determined by ELISA and Lowry assay up to 60 days.

through the BCP nanochannels did not cause physical and chemical denaturation of hGH. Finally, the biological activity of the released hGH was analyzed by ELISA. To compare the bioactivity of the released hGH, the ratio of *in vitro* released hGH concentrations determined by Lowry assay and ELISA was plotted with increasing time (Figure 3d). ELISA data reflect the amount of biologically active hGH, whereas Lowry assay data correspond to the total amount of hGH regardless of the denaturation. Considering the error range of ELISA measurement, the ratios were very close to unity, supporting the intactness of *in vitro* released hGH without denaturation. It was also confirmed by ELISA that the *in vitro* released hGH even after 2 months retained the same biological activity as that of intact hGH.

To demonstrate the feasibility for *in vivo* applications, we investigated the pharmacokinetics of hGH released from a titanium implant drug delivery device with Au-deposited cylindrical nanochannels having a diameter of 6 nm. The drug delivery nanodevice containing 3 mg of hGH in 0.6 mL of PBS was designed for a constant release up to *ca.* 25 days based on *in vitro* release profile of hGH (section 5 in the Supporting Information). Figure 4 shows the pharmacokinetic profile of hGH released from the nanodevice implanted subcutaneously in Sprague–Dawley (SD) rats. For comparison, the pharmacokinetics of hGH was also investigated af-

ter a single subcutaneous injection of 0.1 mg of hGH in 0.4 mL of PBS, which was equivalent to a one day release amount from the implant device. The concentration of hGH in serum was abruptly elevated to a maximum concentration of *ca.* 3000 ng/mL and then dropped to the baseline level within 12 h. On the other

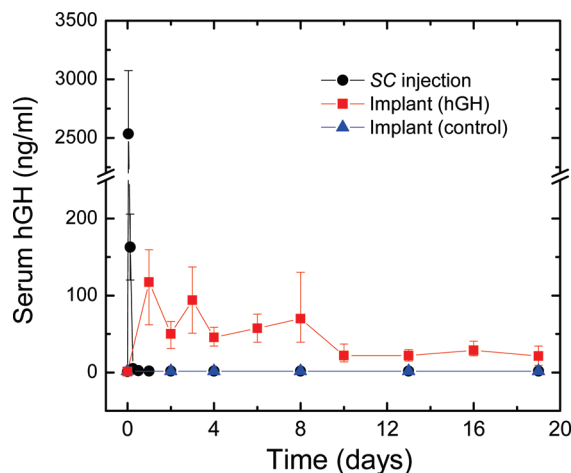


**Figure 4.** Pharmacokinetics of *in vivo* released hGH after a single subcutaneous injection of aqueous hGH (●) and subcutaneous implantation of the titanium device with Au-deposited BCP membrane having a pore size of 6 nm to the SD rats (red rectangle). The drug delivery nanodevice without hGH was used as a control (blue triangle).

hand, the serum concentration of hGH released from the implant device was maintained at a concentration around 50 ng/mL. Depending on the therapeutic range, the release rate (or amount) of hGH can be tuned by changing membrane size in an implant device for further clinical applications. Considering all of these results, the novel protein drug delivery device with cylindrical nanochannels would be successfully applied to the treatment of various chronic diseases with greatly improved patient compliance.

In summary, long-term controlled release of protein drugs by the SFD was successfully demonstrated up to

2 months using the drug delivery device with cylindrical BCP nanochannels. According to the hydrodynamic diameter of a target protein drug, the pore size was precisely controlled down to 6 nm by Au deposition. The release rate of protein drugs could also be controlled by changing the length of BCP nanochannels and the thickness of the Au deposition layer. Due to facile and cost-effective fabrication processes, the drug delivery device with cylindrical BCP nanochannels would be successfully exploited for long-term constant delivery of protein drugs without denaturation for the treatment of various chronic diseases.

## EXPERIMENTAL DETAILS

**Fabrication of Nanoporous BCP Membrane.** PS-*b*-PMMA with an average molecular weight (MW) of 77 000 g/mol and volume fraction of PMMA block of 0.25 was prepared by anionic polymerization. It showed hexagonally-packed cylindrical microdomain with a lattice domain spacing of 35 nm measured by synchrotron small angle X-ray scattering (SAXS). A 2% (w/v) solution in toluene of the mixture of PS-*b*-PMMA and 10 wt % of homopolymer PMMA (30k, Sigma) relative to the PMMA block was spin-coated on a silicon oxide sacrificial layer (~200 nm) deposited wafer with a neutral brush layer and annealed at 170 °C under vacuum for 2 days.<sup>23,26</sup> Then, the film was floated onto the surface of 5 wt % HF solution and then transferred to a microporous membrane support (HT Tuffryn, Pall Life Science). Nanoporous block copolymer membrane was prepared by immersing the block copolymer film floated on the supporting membrane into acetic acid for 1 h, which results in the complete removal of the PMMA homopolymer located at the center of the cylindrical PMMA microdomain. Finally, the nanoporous membrane was dried under vacuum in an oven for 6 h at room temperature. Au was deposited at a rate of 0.1–0.2 Å/s on the top of the nanoporous block copolymer membrane under  $2 \times 10^{-6}$  Torr by using a thermal evaporator. This slow deposition rate of Au could enhance the adhesion between the Au layer and the block copolymer film.<sup>27</sup> The thickness of the Au layer was measured with a quartz crystal piezometry balance. The surface and cross-sectional morphology of the nanoporous membrane was observed by field-emission scanning electron microscopy (FE-SEM, Hitachi S-4600).

**In Vitro Release of Protein Drugs.** BSA and hGH were dissolved in phosphate buffered saline (PBS, pH 7.4) at a concentration of 5 mg/mL. Then, 6 mL of the solutions was put into a test tube with nanoporous membranes and sealed with a cap (Figure S2 in Supporting Information). The delivery device was put into a bath (60 mL) with the fresh PBS. Since only BSA and hGH were diffused out through the membranes, the total solution volume of 6 mL inside the test tubes was maintained during the entire release tests. Before the release test, BCP membrane was soaked in 30% ethanol solution for the better wettability with protein drug solutions. The amount of released BSA and hGH at predetermined times was determined by Bradford protein assay and Lowry assay, respectively. One milliliter of the bath solution was sampled, and the 1 mL of the fresh PBS was added to the bath at each measurement. The intactness of released hGH was checked by RP-HPLC, SDS–PAGE, CD, and ELISA.<sup>28</sup> RP-HPLC was carried out using Vydac\_218MS51\_C4 column at a detection wavelength of 283 nm. The eluent was 0.1 vol % trifluoroacetic acid solution in deionized water/acetonitrile mixture, and the flow rate was 1 mL/min. For SDS–PAGE analysis, the released hGH was mixed with loading buffers containing dithiothreitol and boiled at 90 °C for 2 min. The released protein samples of 24 μL were loaded onto 15% SDS–PAGE gel (8 cm × 8 cm with 1.0 mm thickness). After gel electrophoresis, the gels were stained with Coomassie Brilliant Blue solution. CD spectra for hGH in PBS (pH 7.4) were obtained with a UV spectrophotometer (JASCO J-715)

at 25 °C over the range of 200–250 nm under a nitrogen atmosphere. A quartz cuvette with a path length of 2 mm was used. Raw data were acquired at 0.2 mm intervals with a response time of 1 s. Each spectrum was subtracted by the spectrum of PBS, and the residual ellipticity was calculated as an average of three scans. The bioactivity of released hGH was analyzed with ELISA kits (Diagnostic Systems Laboratory Inc.).

**In Vivo Release of hGH.** Two groups of 3 SD rats (Japan SLC, Hamamatsu, Japan) with a mean body weight of 200 g were used for *in vivo* release test of hGH. For comparison, 0.4 mL of hGH solution at a concentration of 0.25 mg/mL was injected subcutaneously into an SD rat. A titanium device with the Au-deposited BCP membrane was used for *in vivo* release test of hGH (section 5 in the Supporting Information). The drug loading volume was fixed at 0.6 mL. This device was implanted into the subcutaneous tissue of the SD rat. For pharmacokinetic analysis, 0.2 mL of blood samples was collected from lateral tail veins. All blood samples were immediately centrifuged, and the plasma was separated and stored at –20 °C. The serum concentrations of hGH were measured with ELISA kits.

**Acknowledgment.** We thank Shinpoong Pharmaceutical Co. for the kind contribution to *in vivo* release tests. This work was supported by the National Creative Research Initiative Program, the Ministry of Education, Science and Technology (NEST), and Korea Institute for Advancement of Technology (KIAT) through the Human Resource Training Project for Regional Innovation. This research was also supported by the Converging Research Center Program through the National Research Foundation of Korea (NRF) funded by the Ministry of Education, Science and Technology (2009-0081871). Synchrotron SAXS was performed at PLS beam line 4C2 supported by POSCO and NRF.

**Supporting Information Available:** Details on *in vitro/in vivo* release tests of protein drugs and several supporting images. This material is available free of charge *via* the Internet at <http://pubs.acs.org>.

## REFERENCES AND NOTES

- Putney, S. D.; Burke, P. A. Improving Protein Therapeutics with Sustained-Release Formulations. *Nat. Biotechnol.* **1998**, *16*, 153–157.
- Fu, K.; Klivanov, A. M.; Langer, R. Protein Stability in Controlled-Release Systems. *Nat. Biotechnol.* **2000**, *18*, 24–25.
- van de Weert, M.; Hennink, W. E.; Jiskoot, W. Protein Instability in Poly(lactic-co-glycolic acid) Microparticles. *Pharm. Res.* **2000**, *17*, 1159–1167.
- Frokjaer, S.; Otzen, D. E. Protein Drug Stability: A Formulation Challenge. *Nat. Rev. Drug Discovery* **2005**, *4*, 298–306.
- Nishiyama, N. Nanomedicine: Nanocarriers Shape up for Long Life. *Nat. Nanotechnol.* **2007**, *2*, 203–204.
- Zhang, L.; Chan, J. M.; Gu, F. X.; Rhee, J.-W.; Wang, A. Z.; Radovic-Moreno, A. F.; Alexis, F.; Langer, R.; Farokhzad,

- O. C. Self-Assembled Lipid–Polymer Hybrid Nanoparticles: A Robust Drug Delivery Platform. *ACS Nano* **2008**, *2*, 1696–1702.
7. Wu, F.; Jin, T. Polymer-Based Sustained-Release Dosage Forms for Protein Drugs, Challenges, and Recent Advances. *AAPS PharmSciTech*. **2008**, *9*, 1218–1229.
  8. Kukla, V.; Kornatowski, J.; Demuth, D.; Girnus, I.; Pfeifer, H.; Rees, L. V. C.; Schunk, S.; Unger, K. K.; Karger, J. NMR Studies of Single-File Diffusion in Unidimensional Channel Zeolites. *Science* **1996**, *272*, 702–704.
  9. Wei, Q.-H.; Bechinger, C.; Leiderer, P. Single-File Diffusion of Colloids in One-Dimensional Channels. *Science* **2000**, *287*, 625–627.
  10. Chu, W.-H.; Chin, R.; Huen, T.; Ferrari, M. Silicon Membrane Nanofilters from Sacrificial Oxide Removal. *J. Microelectromech. Syst.* **1999**, *8*, 34–42.
  11. Desai, T. A.; Hansford, D. J.; Ferrari, M. Micromachined Interfaces: New Approaches in Cell Immunoisolation and Biomolecular Separation. *Biomol. Eng.* **2000**, *17*, 23–36.
  12. Martin, F.; Walczak, R.; Boiarski, A.; Cohen, M.; West, T.; Cosentino, C.; Ferrari, M. Tailoring Width of Microfabricated Nanochannels to Solute Size Can Be Used To Control Diffusion Kinetics. *J. Controlled Release* **2005**, *102*, 123–133.
  13. Walczak, R. J.; Boiarski, A.; Cohen, M.; West, T.; Melnik, K.; Shapiro, J.; Sharma, S.; Ferrari, M. Long-Term Biocompatibility of NanoGATE Drug Delivery Implant. *Nanobiotechnology* **2005**, *1*, 35–42.
  14. Black, C. T.; Guarini, K. W.; Breyta, G.; Colburn, M. C.; Ruiz, R.; Sandstrom, R. L.; Sikorski, E. M.; Zhang, Y. Highly Porous Silicon Membrane Fabrication Using Polymer Self-Assembly. *J. Vac. Sci. Technol., B* **2006**, *24*, 3188–3191.
  15. Striemer, C. C.; Gaborski, T. R.; McGrath, J. L.; Fauchet, P. M. Charge- and Size-Based Separation of Macromolecules Using Ultrathin Silicon Membranes. *Nature* **2007**, *445*, 749–753.
  16. Liu, G.; Ding, J.; Hashimoto, T.; Kimishima, K.; Winnik, F. M.; Nigam, S. Thin Films with Densely, Regularly Packed Nanochannels: Preparation, Characterization, and Applications. *Chem. Mater.* **1999**, *11*, 2233–2240.
  17. Thurn-Albrecht, T.; Steiner, R.; DeRouchey, J.; Stafford, C. M.; Huang, E.; Bal, M.; Tuominen, M.; Hawker, C. J.; Russell, T. P. Nanoscopic Templates from Oriented Block Copolymer Films. *Adv. Mater.* **2000**, *12*, 787–791.
  18. Kim, J. K.; Lee, J. I.; Lee, D. H. Self-Assembled Block Copolymers: Bulk to Thin Film. *Macromol. Res.* **2008**, *16*, 267–292.
  19. Phillip, W. A.; Rzaev, J.; Hillmyer, M. A.; Cussler, E. L. Gas and Water Liquid Transport through Nanoporous Block Copolymer Membranes. *J. Membr. Sci.* **2006**, *286*, 144–152.
  20. Peinemann, K. V.; Abetz, V.; Simon, P. F. W. Asymmetric Superstructure Formed in a Block Copolymer via Phase Separation. *Nat. Mater.* **2007**, *6*, 992–996.
  21. Lo, K.-H.; Chen, M.-C.; Ho, R.-M.; Sung, H.-W. Pore-Filling Nanoporous Templates from Degradable Block Copolymers for Nanoscale Drug Delivery. *ACS Nano* **2009**, *3*, 2660–2666.
  22. Peng, L.; Mendelsohn, A. D.; LaTempa, T. J.; Yoriya, S.; Grimes, C. A.; Desai, T. A. Long-Term Small Molecule and Protein Elution from TiO<sub>2</sub> Nanotubes. *Nano Lett.* **2009**, *9*, 1932–1936.
  23. Yang, S. Y.; Ryu, I.; Kim, H. Y.; Kim, J. K.; Jang, S. K.; Russell, T. P. Nanoporous Membranes with Ultrahigh Selectivity and Flux for the Filtration of Viruses. *Adv. Mater.* **2006**, *18*, 709–712.
  24. Santini, J. J. T.; Cima, M. J.; Langer, R. A Controlled-Release Microchip. *Nature* **1999**, *397*, 335–338.
  25. Maa, Y.-F.; Hsu, C. C. Investigation on Fouling Mechanisms for Recombinant Human Growth Hormone Sterile Filtration. *J. Pharm. Sci.* **1998**, *87*, 808–812.
  26. Mansky, P.; Liu, Y.; Huang, E.; Russell, T. P.; Hawker, C. Controlling Polymer–Surface Interactions with Random Copolymer Brushes. *Science* **1997**, *275*, 1458–1460.
  27. Cho, J. H.; Jang, Y.; Lee, W. H.; Ihm, K.; Han, J.-H.; Chung, S.; Cho, K. Effects of Metal Penetration into Organic Semiconductors on the Electrical Properties of Organic Thin Film Transistors. *Appl. Phys. Lett.* **2006**, *89*, 132101–132103.
  28. Hahn, S. K.; Kim, S. J.; Kim, M. J.; Kim, D. H. Characterization and *In Vivo* Study of Sustained-Release Formulation of Human Growth Hormone Using Sodium Hyaluronate. *Pharm. Res.* **2004**, *21*, 1374–1381.